AN ANALYTICAL MODEL FOR THE PREDICTION OF DRILLED PILE BASE LOAD-DISPLACEMENT BEHAVIOUR IN COHESIONLESS SOILS

Suthan Pooranampillai, Ph.D., P.Eng
Amec Foster Wheeler Environment and Infrastructure, Edmonton, Alberta, Canada
Sherif Elfass, Ph.D., P.E., Gary Norris, Ph.D., P.E.
University of Nevada - Reno, Reno, Nevada, USA

ABSTRACT
Deep foundations are designed using empirical methods which provide a prediction of shaft base "capacity" dependent on the properties of the surrounding soil/rock material. These capacities are seldom related to a corresponding value of base displacement. To overcome this deficiency, a theoretical model was developed to enable prediction of the load-displacement curve of a drilled shaft base. This model is based on the fundamental concepts of mobilized stress and strain within the soil at the shaft base vicinity. Using information deduced from geotechnical field investigations such as angle of friction and ε_{50} as well as shaft diameter, this model provides predicted load-displacement response of the drilled pile base. The model was compared to published O-cell test results with excellent agreement.

RÉSUMÉ
La méthode empiriques est une façon de concevoir les fondations profonde, cette méthode fournis une prédiction de la «capacité » de la base des puits forée en fonction des propriétés des sols environnantes. Ces capacités sont rarement liées à une valeur correspondante aux déplacements de base. Pour surmonter cette déficience, un modèle théorique a été développé pour permettre la prédiction de la courbe charge-déplacement de puits forée. Ce modèle est basé sur les concepts fondamentaux de la tension et de la pression dans le sol environnant la base des puits forée. À l'aide d'informations des investigations géotechniques collecter en chantier, telles que l'angle de frottement, e_{50} et le diamètre des puits, ce modèle fournit des prédictions de données des charges-déplacement à la base des puits forée. Le modèle a été comparé aux résultats publier de tests O-Cell avec parfaite comparaison.

1 INTRODUCTION

Deep foundations are generally designed based on empirical methods which provide a prediction of "capacity" or "resistance". This capacity assigns a numerical value of possible loading resistance the foundation soils will provide to the foundation structure prior to "failure". Subsequently, a resistance factor (or inversely, a safety factor) needs to be applied to this capacity to assess a secure value up to which loading may be allowed without the danger of "failure". The criterion for such failure is often an unknown quantity (displacement) and is dependent on the definition adopted by the designer on a project by project basis. Currently many engineers adopt a displacement value of 5 percent of pile diameter as permissible for drilled piles with a cut-off at 1 inch displacement.

Reese and O'Neill (1988) provide normalized curves for enabling prediction of base resistance at desired levels of displacement. These normalized curves are based on databases developed from many full – scale load tests carried out on deep foundations. The current LRFD design manual for drilled piles also provides a method for evaluating base displacements based on a desired level of displacement.

Load testing is adopted on especially large or critical projects to obtain the actual load – displacement response of the foundation. Using such load test results, a structurally suitable displacement may be chosen and the resulting foundation resistance obtained from the load – displacement diagram. Such in-situ performance testing enables the designer to re-evaluate the design of the foundation, potentially utilizing higher resistance factors in the subsequent re-design through increased reliability. This will result in lower construction costs.

Provision of a suitably calibrated analytical model, enabling the engineer to predict the load – displacement curve in a variety of soils would substantially simplify design. This would allow the engineer to pick a structurally tolerable level of displacement and anticipate what magnitude of resistance the foundation soil would provide. Such a procedure would be similar to current approaches using Reese and O'Neill (1988) or current LRFD methods, but would be more site specific in that actual parameters such as angle of friction and strain at 50% stress (deduced from field testing) could be utilized such as from SPT "N" value and/or triaxial test results. The model detailed herein will enable the engineer to assess a developing or mobilized net foundation base pressure against displacement, up to full soil failure (true bearing "capacity") throughout the various zones of the failure mass of the model. Full soil failure for all intents may occur at a very high value of displacement. However, since the entire base resistance versus displacement response is provided the engineer may choose a structurally acceptable level of displacement (or desired "failure" criteria) and read off the corresponding resistance from the curve. Additionally, the model will enable the designer to change the strength and strain parameters of the soil and visualize the impact of such changes on the entire load – displacement prediction. Such capability enables the engineer to carry out a sensitivity analysis in the design. This is especially important in geotechnical engineering design given the

empirical nature of many of the correlations involved in utilizing in-situ field testing information.

The numerical model developed and presented in this paper is based on the actual stresses and strains the material at the pile base undergoes. The model converts the stresses applied on the soils at the base and the resultant strain undergone into load-displacement charts. The model is similar to the shallow foundation model developed by Norris et. al (2012).

2 SUMMARY OF THE SHALLOW FOUNDATION MODEL

The bearing resistance of a shallow strip foundation resting in c-ϕ soil is typically assessed based on the well-known bearing capacity equation composed of three terms. These three terms are a function of the pressure caused by the foundation width (B), embedment depth (D) and cohesion (c). Each term has its own bearing capacity factor. There also exist correction factors for foundation shape, embedment, load inclination, load eccentricity and inclination of the foundation base. These correction factors have been substantiated based on model tests but with very few done on realistically dimensioned foundations. Resistance factors or safety factors (up to a magnitude of 3) may be applied on bearing resistance thus calculated to determine factored resistances or allowable bearing pressures. Nevertheless, bearing pressure to limit settlement predominantly governs the design of footings which the traditional bearing capacity equations to do not account for.

2.1 Proposed Model for Prediction of Shallow Foundation Response under Vertical Loading

The proposed model primarily considers the soil providing resistance as made up of three zones/wedges. This is shown in Figure 1. The Mohr circle of stress representing each zone is shown in Figure 2. Herein, zone I is represented by circle I, zone II by circle II and zone III by circle III. From Figures 1 and 2 it becomes apparent that the net ultimate bearing capacity of the foundation is:

$$q_{net} = P_o^* (\tan^6\alpha_f - 1) \quad [1]$$

$$P_o^* = P_o + c/\tan\phi \; ; \; P_o = \tfrac{1}{2} B \, j \, \gamma_y + D\gamma_x \; ;$$

$$j = (1.5 \tan \phi) \quad [2a]$$

$$\alpha_f = 45° + \phi_f /2 \quad [2b]$$

where ϕ_f is the friction angle at failure. The equation for a given mobilized condition is:

$$q_{net,\,m} = P_o^* (\tan^6\alpha_m - 1) \quad [3a]$$

$$\alpha_m = 45° + \phi_m/2 \quad [3b]$$

where ϕ_m is the friction angle of a mobilized state. Equations relating ϕ_m to ϕ at a specified stress level (SL) is as follows:

$$\sin \phi_m = SL*A/(SL*A +2) \; ;$$
$$A = \tan^2(45+\phi/2) - 1 = 2 \sin \phi / (1- \sin \phi) \quad [3c]$$

All three zones are assumed to be at the same stress level ($SL = \sigma_{dm}/\sigma_{df}$), though strains will differ. The mobilized friction angle ϕ_m at any given stage of loading can be represented in terms of the stress level of the soil as well as the friction angle of failure of the soil.

Foundation displacement ρ is directly related to the peak vertical or major principal strain ε of zone III representing the peak of the Schmertmann strain triangle over depth 2 times the width of the foundation.

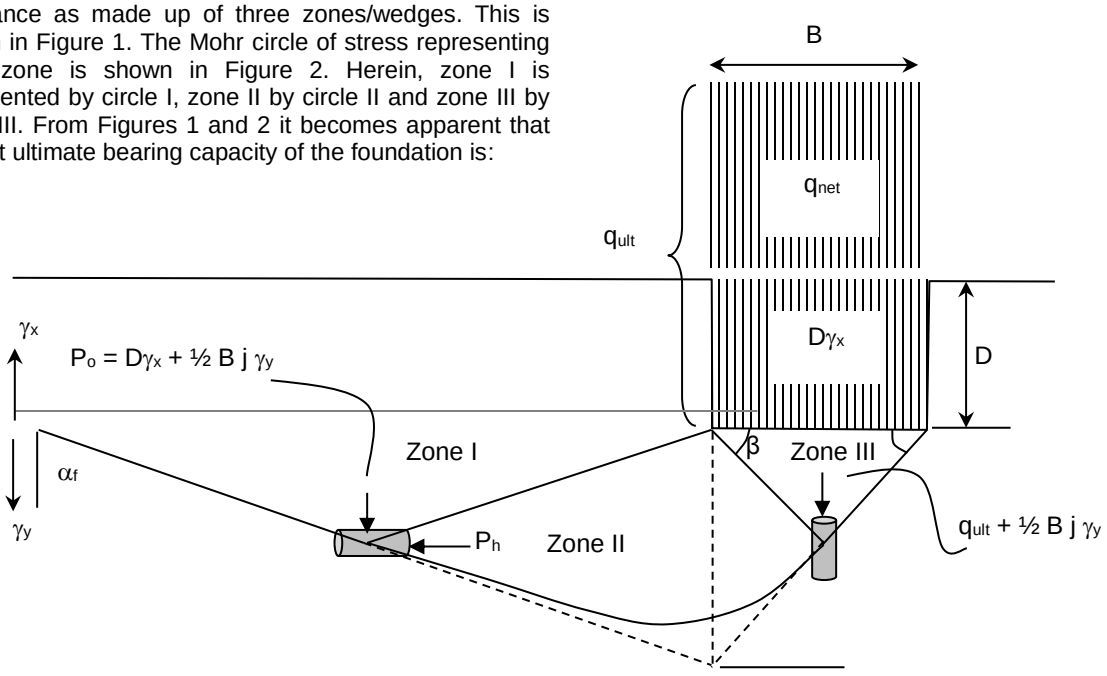

Figure1: Three wedge model of the developing failure mass of a shallow foundation

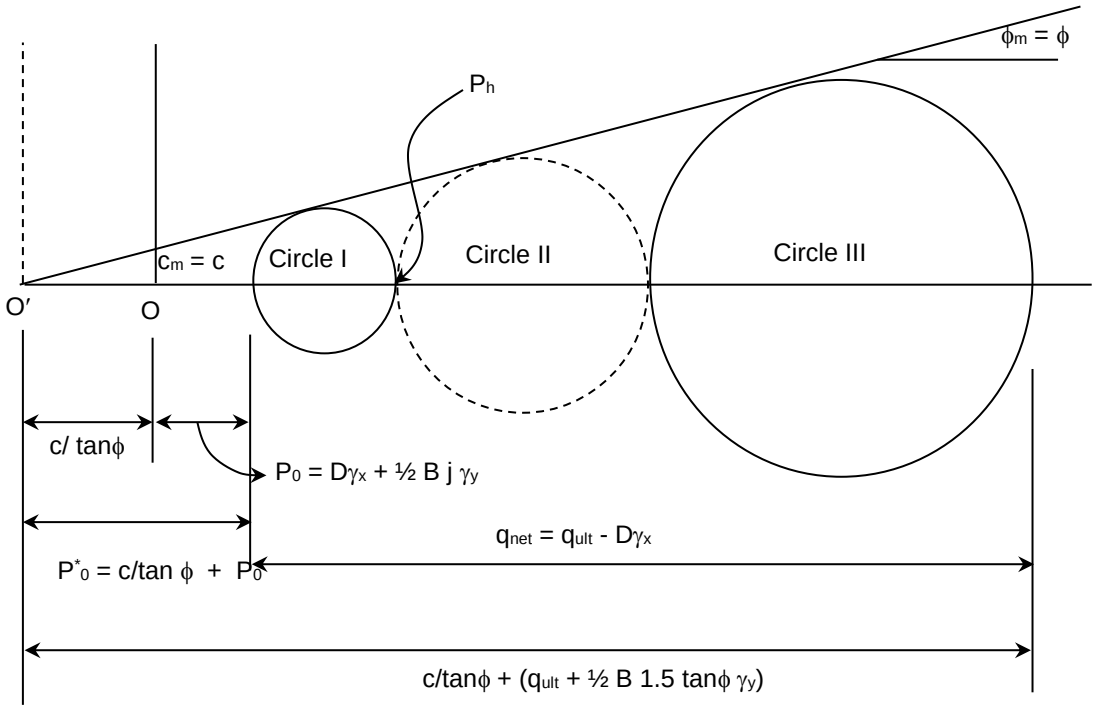

Figure 2: Mohr circle representation of the three zones

Note that:

$$\varepsilon = \sigma_{dm} / E \qquad [4]$$

where $\sigma_{dm} = \Delta\sigma'_1 - \Delta\sigma'_3$ of zone III and E is the secant Young's modulus of the soil that corresponds to the current confining pressure of zone III.

The confining pressure in zone III continually changes as the applied pressure ($q_{net,m}$) at the base of the foundation or the top of the soil of zone III increases. The changes in major and minor principal stresses for the different zones can be established from P_o* using trigonometry or graphical construction (see Figure 2) based on ϕ_m (for a specified SL in Eq. 3c) that, in turn, yields $q_{net,m}$.

The total displacement ρ at any $q_{net,\,m}$ is equal to the area of the strain triangle or εB (= ε* ½ * 2B). The strain ε can be assessed from the following relationship:

$$\varepsilon = SL \frac{e^{3.707\,SL}\varepsilon_{50}}{\lambda} \qquad [5a]$$

where SL is the stress level present in the soil (= σ_{dm}/σ_{df}). The deviatoric stress in each soil zone is σ_{dm} which can be represented in terms of the confining pressure of that zone at any given moment (bearing in mind that confining pressure in zones II and III change as loading is applied). The representation of σ_{dm} at failure (i.e. σ_{df}) in terms of confining pressure is:

$$\sigma_{df} = A\,\sigma_3' \qquad [5b];$$

with A given by Eq. 3c

ε_{50} is the strain when SL = ½. The ε_{50} of the soil is generally estimated from triaxial tests conducted at constant confining pressure. This ε_{50} can also be determined from correlation based on Figure 3 for siliceous sands. The confining pressure in Figure 3 or that of the triaxial tests will be different from the changing confining pressure encountered in the zone III. Correction for the current confining pressure in zone III can be approximated (Ashour and Norris, 1998) as:

$$\varepsilon_{50} = \varepsilon_{50,ref} (\sigma_3'/\sigma_3'_{ref})^{\,n} \quad ; \; n = 0.2 \text{ to } 0 \qquad [5c]$$

where $\sigma_3'_{ref}$ is 0.87 ksf, if using Figure 3, or the confining pressure of the triaxial test closest to the current value of σ_3' of zone III.

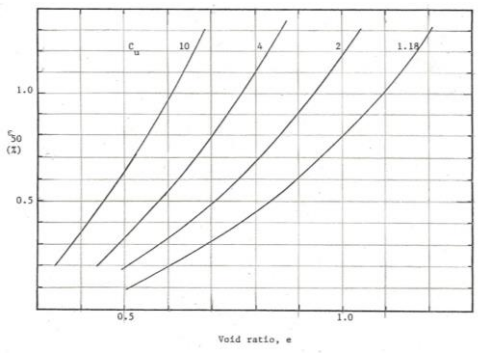

Figure 3: ε_{50} at 0.87 ksf, a function of e and C_u (modified from Ashour and Norris,1988)

λ of Equation Eq. 5 is a function of SL. This is presented by Ashour and Norris (1998) with an updated version of it given in Norris et. al. (2012) as follows:

$$\lambda = 3.19 \text{ for SL} < ½ \qquad [5d]$$

$$\lambda = -7.1219\,SL^2 + 7.0592\,SL + 1.4403 \text{ for SL} > ½ \qquad [5e]$$

3 REFINEMENT OF THE SHALLOW FOUNDATION MODEL FOR APPLICATION IN DEEP FOUNDATION ANALYSIS

3.1 Impact of Side Shear Load on Overburden Pressure at the Foundation Base

The predominant difference between deep foundations and shallow foundations is the depth of the base of the foundation. The depth to the base of the deep foundation exposes a large area of the foundation sides to soil that is not prevalent in the shallow foundation. This results in a large amount of side shear on the deep foundation that is not present in shallow foundations. The effective overburden pressure P_o^* (= $c/\tan\phi + D\gamma_x + \frac{1}{2} Bj\gamma_y$) or minor principal stress of zone I of the shallow foundation model, is unaffected by any side shear of the shallow foundation while this is not the case with a deep foundation. As shown in Figure 4a, the downward movement of the pile and associated concentric cylinder of mobilized soil of diameter ($B+ 2f_m$) generates a side shear force along the circumference of the soil cylinder. This side shear force acting on the circumferential area of the soil cylinder causes a reduction (ΔP_o^*) in effective overburden pressure or minor principle stress of zone I taken over the annular area ($\pi[(B+2f_m)^2 - B^2]/4$) of the soil cylinder. In turn, this results in a somewhat smaller mobilized net pressure ($q_{net,m}$) of the pile base than had there been no ΔP_o^* reduction. See Figures 4a and 4b. As a consequence, load induced side shear affects the mobilized end bearing resistance and should be considered as part of the analysis. In effect, mobilized end bearing and side shear resistances should really be considered as a unit, at least over the height/length ℓ_m over which such interaction occurs. Note that the side shear force over the perimeter of the diameter ($B+2f_m$) is equal to the side shear force Q_s at the pile/soil interface of diameter B, i.e.

$$\tau_{(B+2fm)/2}\ \pi\ (B+2f_m)\ = \tau_{B/2}\ \pi\ B\ = Q_s \qquad [6]$$

As an approximation, the mobilized value of ℓ can be taken as

$$\ell_m = f_m/\tan\phi \qquad [7]$$

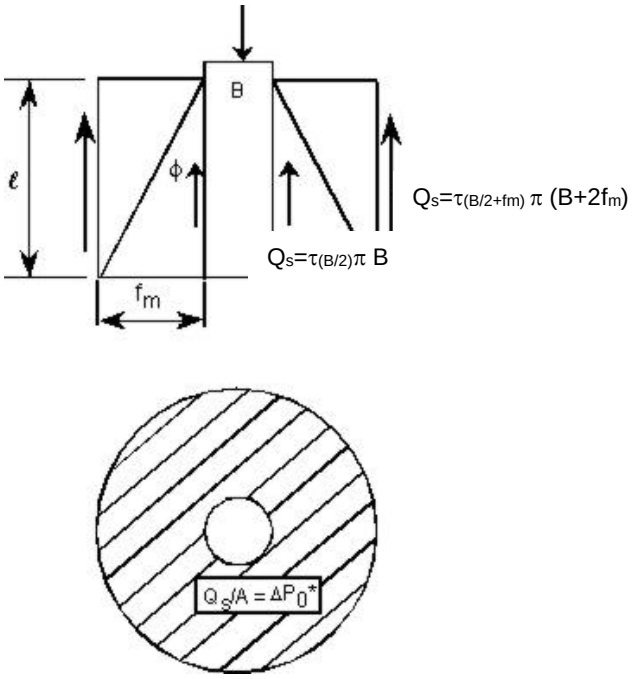

Figure 4a Downward movement of pile mobilizes concentric cylinder of soil

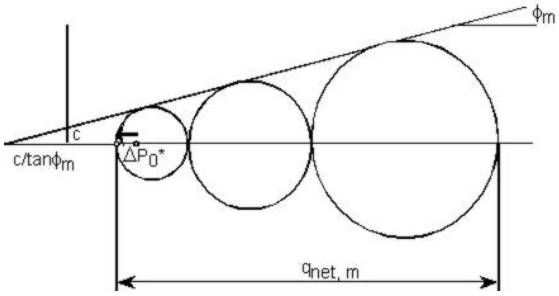

Figure 4b Mohr-Coulomb diagram showing effect of a reduction in confining pressure

Note that in the above discussion, f_m is a mobilized distance that is a function of the mobilized friction angle (ϕ_m) of the base foundation model as characterized by a standard triaxial test stress state response. On the other hand, the side shear response is a function of the more quickly mobilized side shear resistance which peaks much earlier than the base response. Such side shear response can be modeled, as is done with side shear response in the Strain Wedge model ($\tan\phi_{ss,m} = 2\tan\phi_m < \tan\phi$), with further modification for a lower interface friction than pure soil friction response, i.e. $\tan\delta_m$ is:

$$\tan\delta_m = \tan\phi_{ss,m}\ (\tan\delta/\tan\phi) \qquad [8a]$$

There is one other concern relative to a reduced P_o^* due to ΔP_o^*. The reduction discussed above is due to loading of the pile and its value increases up to a maximum reduction ΔP_o^*at the moment side shear peaks, i.e. $\delta_m = \delta$ where:

$$\tan \delta = \tan \phi_{ss,m} \ (\tan \delta / \tan \phi); \ \phi_{ss,m} = \phi \qquad [8b]$$

i.e. $\phi_{ss,\,m}$ reaches its limiting value (the same as peak resistance of soil in zone I, with minor adjustment for overburden pressure difference at l/2 above the base, assuming the soil along the pile sides is the same as in zone I).

There is, however, the possibility of an added component of reduction ΔP_o^* due to installation effects. This is why, for driven piles, the vertical effective stress at the pile base is traditionally limited to a value of some critical depth (say at 20 pile diameters).

3.2 Model Response and Solutions

The model is an effective stress (ES) analysis that assesses pile base movement as a function of strain immediately beneath the foundation base of width B similar to the shallow foundation model. Therefore, the strain of interest occurs in zone III. The strain is characterized by standard axial compression triaxial test response, with the exception that the minor principal stress of zone III (equal to the triaxial test confining pressure) is changing with increasing applied base pressure $q_{net,m}$. This is accommodated from triaxial results as if at the different mobilized deviatoric stress ($\sigma_{dm,\,III}$), the soil is moving from one triaxial test confining pressure ($\sigma'_{3,\,m}$) curve to another, as indicated in Figures 5 a and b. The displacement of the base of the foundation (ρ) is assessed from Schmertmann's square/round 2B strain triangle of peak ε_1. This base displacement is equal to the triaxial test axial strain at a deviatoric stress within zone III of $\sigma_{dm,III}$ at the current effective confining pressure of wedge III, i.e. $\rho = \varepsilon_1 B$.

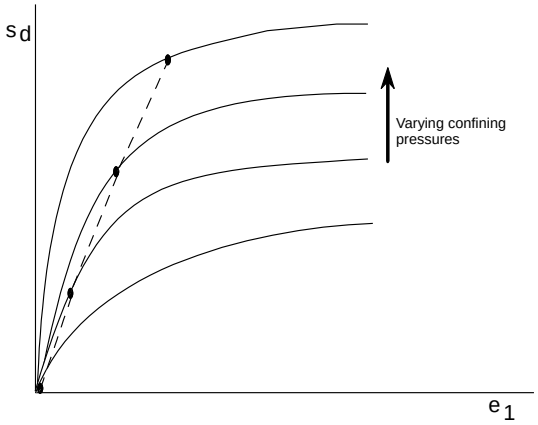

Figure 5a: Change in confining pressure of zone III and corresponding σ_{dm} and ε

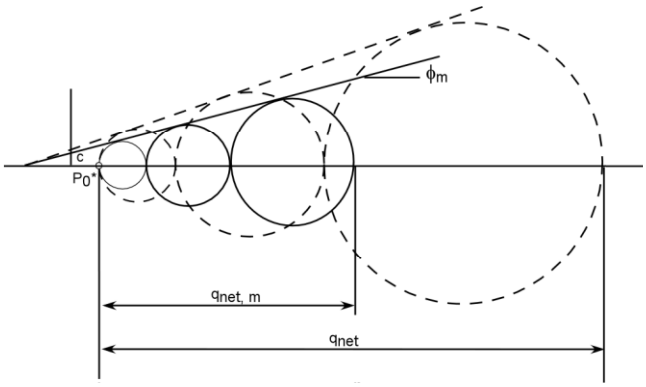

Figure 5b: Changing stress state with increasing applied pressure $q_{net,m}$

Such drained triaxial test stress-strain (σ_d - ε_1) response (at a given σ'_3) has been characterized previously as SL vs ε as given by Eq. 5 (a – e).

Likewise, the peak values of the secant friction angle of Mohr circles of zones II and III vary with the current confining pressure σ'_3 of wedges II and III, as per a modified version of Bolton's equation (Elfass and Norris, 2012) which yields $\Delta\phi$. $\Delta\phi$ is the decrease in peak secant friction angle per log cycle change in effective confining pressure, which can be evaluated given a reference value ϕ_{ref} at a reference pressure $\sigma_{3,ref}$ and knowledge of the relative density (D_r) of the sand. Based on the peak friction angle ϕ, the associated mobilized friction ϕ_m is given by Eq. 3c based on the SL considered.

3.3 Spreadsheet

A spreadsheet was developed to carry out the calculations. This model provides the variation in base resistance with displacement. The spreadsheet calculates resistance as;

$Q_b = q_{net,\,m}\, A$ (A = base area)
Displacement as $\rho = \varepsilon\, B$ (B = Pile Diameter)

The model response evaluation, requires the following input:

a. Cohesion (c) and peak friction angle (ϕ) at σ_{3ref}
b. Relative density (D_r), which yields $\Delta\phi$ and ϕ_{min} (whereby $\phi = \phi_{ref} - \Delta\phi \log (\sigma'_3/\sigma'_{3,ref}) > \phi_{min}$)
c. δ for side shear evaluation and hence ΔP_o^*
d. $P_o^* = c/\tan\phi + D\gamma_x + \frac{1}{2} Bj\gamma_y$; $j = 1.5 \tan\phi$

3.4 Assessing ϕ and ε_{50} for Use in the Analytical Model

The foremost necessity for model analysis is a ϕ_{ref} at a reference pressure $\sigma_3'_{ref}$. $\sigma_3'_{ref}$ together with $\Delta\phi$ (which can be assessed from Bolton's equation knowing ϕ_{ref} and D_r) are then used to assess the secant ϕ in each zone based on the current σ_3' in that zone. While it would seem that ϕ_{ref} would best be obtained from the triaxial test on an undisturbed sample, including tests at different σ_3' to assess $\Delta\phi$ directly. However this is not likely to be undertaken in regular design work due to the necessity of obtaining undisturbed samples from the field (a virtual impossibility in cohesionless material) and the likely variable soil conditions (changes in short depths). Therefore, on a realistic basis, it is the in-situ field test that must be used to assess a value of ϕ, and this requires appropriate interpretation. For instance, based on an N_{60} blow count from the standard penetration test (SPT) and charts from DM 7 page 7.1-14 or 7.1-87 and 7.1-149 and a ϕ_{ref}, or a range in ϕ_{ref} values, can be assessed corresponding to an assumed $\sigma_3'_{ref}$ of, say, one ton per square foot. In lieu of triaxial tests, $\varepsilon_{50,ref}$ at a pressure $\sigma_3'_{ref}$ of 0.87ksf pressure can be estimated from Figure 3.

4 CASE STUDIES

Towards evaluating the applicability of the numerical model described previously, two case studies were investigated. Due to the need to evaluate the base response separate from the shaft top response, Osterberg Cell (O-Cell) load tests were needed as opposed to standard top down static load tests. Therefore tests incorporating the O-Cell procedure were utilized. Both the studies documented herein were carried out to evaluate the suitability of the proposed model in producing pile base load – displacement response similar to actual recorded data.

4.1 Case Study 1: 9 - Foot Diameter Drilled Pile at Cranston Viaduct

The information used in this study was obtained from Mohammed and Armfield (2004). The Cranston Viaduct test pile was constructed to compare evaluations provided by different design methods with actual field test data for both side shear and base resistance prediction.

Soil borings indicated that the bottom 50 feet of the sand stratum encountered, which is present down to the maximum explored depth, consisted of brown compact fine sand with a little silt. The average Standard Penetration Resistance N-values recorded during the investigation ranged from 27 blows to 55 blows per foot. Design values for the angle of internal friction were estimated during the design stage as varying between 33 and 36 degrees. The ground water was recorded as varying between 15 to 20 feet below existing surface level.

Construction of the 9-foot diameter drilled pile was carried out using a temporary casing near ground surface to prevent collapse as well as a permanent casing down to 30 feet below ground surface. Polymer slurry was introduced into the hole for stability of the bottom portion of the hole and termination of drilling of the pile boring was at depth of 133.5 ft. Thereafter the pile reinforcement was installed together with the Osterberg Cell (O-Cell) load test assembly. The O-Cell was placed 18.5 feet above the base of the pile.

For input into the model, three different pairs of ϕ_{ref} and $\varepsilon_{50,ref}$ were used. This was done to show the possible variation in the load – displacement curve. For this case study the following additional parameters were utilized: γ_x = 0.071 kips/ft^3, γ_y = 0.057 kips/ft^3, δ/ϕ = 0.5, and depth of pile base D = 133.5 ft. Additionally, the length of the effective point of action of the base (for Q_t in model analysis) at ℓ_m was assigned as fixed at 18 ft. since the O-Cell was placed 18 ft. above the base. The analysis was carried out by changing ϕ_{ref}. For an angle of 33^o, $\varepsilon_{50,ref}$ = 0.0475 and a relative density of 60% was utilized. For the second run an angle of 36^o together with $\varepsilon_{50,ref}$ = 0.03 and relative density of 70% was employed. For the third analysis an average angle of 34.5^o together with $\varepsilon_{50,ref}$ = 0.0425 and relative density of 65% was utilized. The very high values of $\varepsilon_{50,ref}$ were deemed necessary due to likely presence of slurry and/or slough trapped below the pile base. There was no reported evaluation of the end conditions for this test. On the other hand, load resistance would be governed by the sand and at some large displacement the slurry/slough would compress and deformation would also revert to purely a sand response.

Results from these trials are plotted against the recorded response in Figure 6. The "capacity" of the pile can be seen to vary depending upon the chosen displacement. If an allowable displacement of 1.5 inches is used (1.4% of pile diameter) the model predicts a value (at ϕ_{ref} of 34.5^o) of base resistance of approximately 2500 kips that matches the field observation. At 5.4 inches (5%) displacement, the 33^o model trial slightly over predicts the field value (if the field curve were to be extended). Alternatively, Reese and O'Neill (1988) predict 32 - 66 ksf (1.2 * N) base resistance for SPT values 0 - 75 (as observed in this case below the pile base) for 5% displacement. This gives a base resistance value of 2060 - 4200 kips. This is a fairly large range. To this the 18 ft. of

side shear load from the base to the O – Cell location would also need to be added.

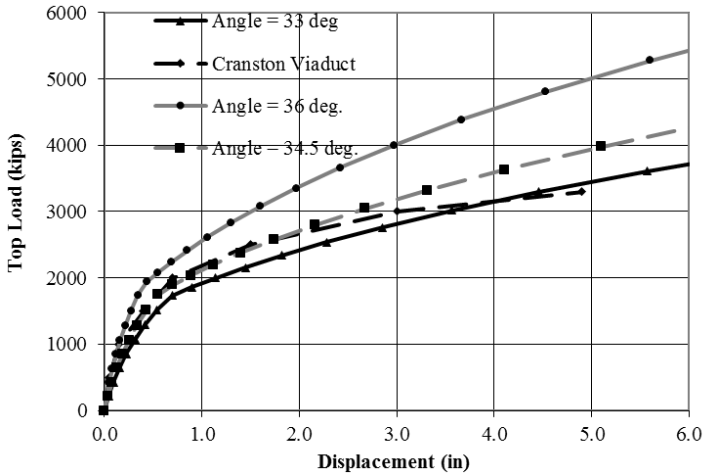

Figure 6: Model predicted vs. recorded response, Cranston Viaduct

4.2 Case Study 2: Osterberg Load Cell Test Results on Bored Piles in Bangladesh

The information used in this study was obtained from Castelli and Wilkins (2004). The load test piles were constructed as part of a test pile program conducted to ascertain performance of foundations constructed for the Paksey Bridge crossing the Padma (Ganges) River in Bangladesh. Two test piles were constructed with O-Cells installed at the bas as well as along the length of the pile.

Existing subsurface soils at the pile base elevation were generally very dense micaceous, silty, medium to fine sand with occasional zones containing trace amounts of fine gravel. Standard penetration test N-values were generally greater than 100 blows per foot. Although the soils are very dense, a conservative friction angle of 36 degrees was assumed for design due to the high mica content (as high as 26%).

Construction was carried out using bentonite slurry. De-sanders were used during drilling to clean the bentonite. Concrete was mixed on-site for its use in the construction. The test pile was approximately 225.5 ft. deep and 5 ft. in diameter. O-Cell testing was carried out on both grouted as well as ungrouted test piles. The O-Cell was placed at l_m of 4.8 feet above the base of the pile. Another O-Cell was placed a further 50.8 feet above the lower O-Cell. The arrangement of the two O-Cells was to determine the load – displacement behavior of the pile side shear resistance between the two O-Cells.

The “capacity” of the pile can be seen to vary depending on the chosen displacement. If an allowable displacement of 1.0 inch is used (1.7% of pile diameter) the initial analysis model predicted value of approximately 1080 kips closely matches the field observation of 1050 kips for the $\phi_{ref} = 36^o$ (in Figure 7). The $\phi_{ref} = 33^o$ prediction gives a value of 800 kips at this same displacement. It was not possible to compare the measured response with the model

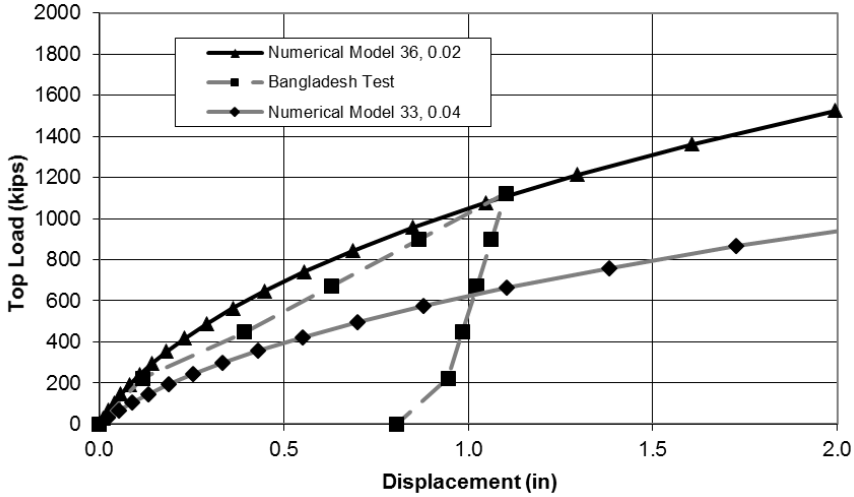

Figure 7: Model predicted vs record response, bored Piles in Bangladesh

response beyond 1.1 inch displacement due to the lack of data.

5 CONCLUSIONS AND RECOMMENDATIONS

The proposed model provides agreement within range for the two case histories considered here. This model was also shown to provide agreement with the results of large scale laboratory tests conducted in a controlled soil density environment (test results found in Pooranampillai et al. 2009, 2010).

This model provides the designer with a tool, whereby the full range of drilled pile base load-displacement behavior may be modeled. Additionally, by allowing the designer to vary the soil properties this model allows a sensitivity analysis to be carried out.

6 NOTATIONS

Symbol	Description
A	Cross-sectional area of pile
B	Pile diameter,
c	Cohesion
c-ϕ	Soil possessing both cohesion and friction
D	Embedment depth of base of pile,
D_r	Soil relative density
E	Secant Young's modulus of soil
e_{max}	Maximum void ratio of a soil type
e_{min}	Minimum void ratio 0f a soil type
f_m	Distance from wall of pile to outermost soil cylinder mobilized during loading
F_s	Ultimate side shear resistance
j	1.5 tan ϕ
l_m	Mobilized height of pile/soil interaction from base of pile
P_o	Effective overburden pressure at depth under consideration
P_o* (or P_0 +c/tanϕ)	Effective overburden pressure as a pure ϕ soil from new origin at O' shifted on X-axis by c/tanϕ
ΔP_o*	Reduced overburden pressure at depth under consideration
Q_b	Mobilized base resistance
Q_s	Side shear force at pile/soil interface immediately above pile base
Q_{sm}	Mobilized side shear between base of pile and level of loading resistance measurement
q_{net}	Net ultimate bearing capacity of foundation
$q_{net,m}$	Net mobilized bearing capacity
SL	Stress level
α_m	45° + ϕ_m/2
α_f	45° + ϕ /2
$\Delta\phi$	Change in peak friction angle per log cycle change in confining pressure
ε	Axial strain in soil immediately below base of pile
ε_{50}	Strain at 50% stress level
$\varepsilon_{50,ref}$	Strain at 50% stress level at reference pressure
ε_1	Axial strain in triaxial testing
ε_f	Failure strain
σ'_3	Confining pressure
σ_d	Deviatoric stress during triaxial testing
σ_{dm}	Mobilized deviatoric stress
σ_{df}	Deviatoric stress at failure
δ_m	Mobilized friction angle at soil/pile interface
δ	Friction angle at soil/pile interface at failure
$\sigma_{3\,ref}$	Reference confining pressure
ϕ	Angle of internal friction at failure
ϕ_{ref}	Angle of internal friction at reference pressure
ϕ_m	Mobilized angle of internal friction
$\phi_{ss,\,m}$	Mobilized friction angle for pile side shear
λ	A variable which is a function of stress level
ρ	Pile displacement
γ_x	Unit weight of soil mass above base level
γ_y	Unit weight of soil mass below base level

7 REFERENCES

CASTELLI, R., WILKINS, E., 2004. Osterberg Load Cell Test Results on Base Grouted Bored Piles in Bangladesh. Geosupport 2004. Drilled Shafts, Micropiling, Deep Mixing, Remedial Methods, and Specialty Foundation Systems. American Society of Civil Engineers, Geotechnical Special Publication Number 124. Pp 587 – 602.

ELFASS, S., NORRIS, G., 2008. Undrained Tip Response of Drilled Piles in Cohesionless Material. Geotechnial Earthquake Engineering and Soil Dynamics. IV. American Society of Civil Engineers, Geotechnical Special Publication Number 186

MOHAMMED, A. M. and ARMFIELD, K. C., 9-foot diameter drilled shafts at Cranston Viaduct: Design, Load Testing and Construction, GeoSupport 2004.

POORANAMPILLAI, J., ELFASS, S., VANDERPOOL, W., NORRIS, G., 2009. Large-Scale Laboratory Study on the Innovative use of Compaction Grout for Drilled Shaft Tip Post Grouting. Contemporary Topics in Deep Foundations. American Society of Civil Engineers Geotechnical Special Publication Number 185, pp 39 – 46.

POORANAMPILLAI, J., ELFASS, S., VANDERPOOL, W., NORRIS, G., 2010. The Effects of Compaction Post Grouting of Model Shaft Tips in Fine Sand at Differing Relative Densities – Experimental Results. Art of Foundation Engineering Practice – GSP honoring Clyde Baker. American Society of Civil Engineers Geotechnical Special Publication Number 198, pp 486 – 500.

POORANAMPILLAI, J., ELFASS, S., VANDERPOOL, W., NORRIS, G., 2010 (in press). Large Scale Laboratory Testing of Low Mobility Compaction Grouts for Drilled Shaft Tips. Geotechnical Testing Journal.

REESE, L., C., O'NEILL, M. W. (1988). Drilled Shaft Construction and Design. FHWA Publication No. HI-88-042.